

Article

# Determination of the Structural Characteristics of Microalgal Cells Walls under the Influence of Turbulent Mixing Energy in Open Raceway Ponds

Haider Ali <sup>1</sup> , Taqi Ahmad Cheema <sup>2</sup> and Cheol Woo Park <sup>1,\*</sup> 

<sup>1</sup> School of Mechanical Engineering, Kyungpook National University, Daegu 41566, Korea; haider7771@hotmail.com

<sup>2</sup> Department of Mechanical Engineering, GIK Institute of Engineering Sciences and Technology, Topi 23460, Pakistan; taqi\_cheema39@hotmail.com

\* Correspondence: chwoopark@knu.ac.kr; Tel.: +82-53-950-7569

Received: 11 January 2018; Accepted: 6 February 2018; Published: 7 February 2018

**Abstract:** Turbulent flow mixing is essential in optimizing microalgal cultivation in raceway ponds. Microalgal cells are however highly sensitive to hydrodynamic stresses produced by turbulent mixing because of their small size. The mechanical properties (wall deformation and von Mises stress) of the microalgal cell wall structure under the influence of turbulent mixing are yet to be explored. High turbulence magnitudes damage microalgal cell walls by adversely affecting their mechanical properties which consequently destroy the microalgal cells and reduce the biofuel production. Therefore, such a study is required to improve the biofuel productivity of microalgal cells before their cell wall damage in raceway pond. This study developed a novel fluid–structure interaction (FSI)-based numerical model to investigate the effects of turbulent mixing on the cell wall damage of microalgal cells in raceway ponds. The study investigated microalgal cell wall damage at four different locations in a raceway pond in consideration of the effects of pond’s hydrodynamic and geometric properties. An experiment was conducted with a laboratory-scale raceway pond to compare and validate the numerical results by using time-dependent water velocities. Microalgal cell wall shear stress, cell wall deformation, and von Mises stress in the raceway pond were investigated by considering the effects of aspect ratios, water depths, and paddle wheel rotational speeds. Results showed that the proposed numerical model can be used as a prerequisite method for the selection of appropriate turbulent mixing. Microalgal cell wall damage is high in shallow and narrow raceway ponds with high paddle rotational speeds.

**Keywords:** raceway pond; turbulent mixing; microalgal cell wall damage; FSI; wall deformation

## 1. Introduction

Turbulent flow mixing prevents the sedimentation of microalgal cells in raceway ponds, facilitates removal of the oxygen, and increases the interaction of microalgal cells with sunlight and carbon dioxide. Turbulence also reduces the boundary layer around microalgal cells, and this reduction increases the diffusion rate of nutrients to the cell surface [1–4]. Turbulent mixing can be increased by increasing the paddle wheel speeds. However, microalgal cells are highly sensitive to fluid stresses because of their small size, and high turbulence magnitudes can damage their cell walls [5–8]. Numerous studies have investigated the impact of turbulence on algal growth to establish optimal relationship in order to improve biomass production. An increase in the water depth increases the water volume of the raceway pond which in return reduces the water circulation velocity. This reduction in the water velocity results in an ineffective turbulent mixing that consequently reduces the interaction of microalgal cells with sunlight, carbon dioxide, and nutrients [9]. Turbulent mixing can be increased

in the deep raceway pond (large water depth) by increasing the paddle wheel speed (water velocity), but this increases the power consumption [10]. Algal productivity increases about 2.5% when the water depth of the raceway pond decreases to half, attributed to the effective turbulent mixing [9,11]. The sunrise and the sunset hours are more critical in terms of the algal productivity because the level of oxygen increases in the raceway pond during these time periods. Turbulent mixing is particularly important during sunrise and sunset hours, since the algal productivity of turbulent water is approximately twice that in non-turbulent water because of the removal of oxygen from the raceway pond [9,12,13]. Numerous studies have reported controversial data. Several have reported that an increase in water turbulence (Reynolds number = 7370–221,160) negatively affects algal productivity, whereas others have indicated that no change in productivity occurs. Previous studies by Weissman et al. [10], Drapcho [14], and Grobbelaar [15] have reported that algal productivity increases up to a certain turbulence range, and further increasing the turbulence exerts a negligible effect on microalgal growth [10,14,15]. Therefore, it can be inferred that the reduced productivity reported in the aforementioned studies could be result of microalgal cell wall damage because of the use of turbulence of high magnitude [10,14,15]. Therefore, as a prerequisite, the effects of selected turbulence on the cell wall of microalgal cells must be evaluated to ensure that microalgal cells are not damaged in the process. Only then can an acceptable relationship be established between turbulence and algal productivity.

Investigation of the effects of turbulence on microalgal cell damage has recently become a topic of interest for numerous researchers. Thomas and Gibson [16] used fluid mechanical properties (dissipation rate, microeddy length, and shear stress) to observe the effects of turbulence on different microalgal species. The paddle wheel must generate microeddies with a length larger than the cell size to avoid damaging the microalgal cell [16–18]. Increasing the agitation rates also increases the hydrodynamic stresses that affects the algal cell damage [17,19,20]. Hadiyanto et al. [21] used a commercial computational fluid dynamics (CFD) code to model hydrodynamic mixing in a raceway pond. Microalgal cells were not included in the CFD model, and the cell damage was investigated by estimating the fluid properties (microeddy length and shear stress) [21]. Previous studies are limited because microalgal cell damage was examined by computing and comparing the turbulence flow parameters, but the microalgal cell wall was not investigated. A cell wall is a structural layer, surrounding microalgal cells, that provides the components of the cell (cytoplasm, nucleus, etc.) with structural support and protection from the external environment. The cell wall is a mechanical structure because it has a considerable tensile strength (elastic modulus = 8.5 MPa) [22]. Large hydrodynamic stresses damage the cell wall, leaving the cell components exposed to the external environment. This damage of the cell wall destroys the microalgal cell and reduces the algal productivity. Therefore, the mechanical properties (wall deformation and von Misses stress) of the cell wall must be estimated to investigate the effects of turbulence on microalgal cell damage [23]. The authors previously used CFD particle tracing to investigate the turbulent mixing of microalgal cells in a raceway pond [24]. However, the study focused on the evaluation of mixing phenomena and disregarded the effects of turbulence on microalgal cell wall damage. Turbulence varies in different sections of raceway ponds, and microalgal cells near the paddle wheel experience larger flow stresses than those experienced by cells in the downstream channel. Turbulence mixing depends on paddle wheel speed and geometrical features (channel depth and width), so microalgal cell wall damage is also affected by these parameters [25]. Therefore, a study involving the modeling of the mechanical structure (cell wall) of microalgal cells in raceway pond in consideration of the effects of water turbulence must be conducted to estimate microalgal cell damage effectively and achieve improved microalgal productivity [11].

The aim of this study is to develop a novel fluid–structure interaction (FSI)-based numerical model to investigate the influence of water turbulence on microalgal cell wall damage in raceway ponds. The present study predicted the effect of water turbulence on the cell wall structure of a unicellular and spherical algal species (*Chlorella*). Cell wall damage was investigated by estimating the mechanical

properties of the microalgal cell wall. The arbitrary Lagrangian–Eulerian (ALE) method was used to model the effects of water turbulence on the cell wall of microalgal cells [26,27]. Microalgal cell wall damage was estimated at four important locations in a raceway pond (Figure 1a). The effects of the pond’s hydrodynamic and geometric properties on microalgal cell wall damage were also considered. The CFD model was validated by using the experimental results of water velocity obtained from a laboratory-scale raceway pond. Various pond aspect ratios, water depths, and paddle wheel rotational speeds were investigated to examine their effects on cell wall shear stress, wall deformation, and von Mises stress at different locations in the raceway pond. This study helps in optimizing the power requirement of the paddle wheel to induce the required turbulent mixing without affecting the microalgal cell wall.

## 2. Materials and Methods

### 2.1. Geometries of the Raceway Pond and Microalgal Cells

The geometrical model of a commercial 3D raceway pond was constructed in the COMSOL-Multiphysics (5.3, COMSOL Inc., Burlington, MA, USA). The pond had a length ( $L$ ) of 23 m and a channel width ( $W$ ) of 2.25 m (Figure 1a). A 2D paddle wheel with six blades ( $0.55\text{ m} \times 0.04\text{ m}$ ) and a diameter of 0.6 m was used to circulate water in the 3D raceway pond. The boundary-connected coupling method was employed to introduce the pulsatile flow of the 2D paddle wheel in the 3D raceway pond [24,28–30]. The Reynolds number ( $Re_h$ ) based on the hydraulic diameter ( $D_h$ ) determined the turbulent flow in the raceway pond as follows:

$$Re_h = (\rho_l D_h U_l) / \mu_l \quad (1)$$

$$D_h = 4WH / (2H + W) \quad (2)$$

where  $W$  and  $H$  are the width and height of the pond, respectively;  $\rho_l$  is the water/liquid density ( $1000\text{ kg/m}^3$ );  $\mu_l$  is the water viscosity ( $0.001\text{ Pa}\cdot\text{s}$ ); and  $U_l$  represents the average water velocity (m/s).

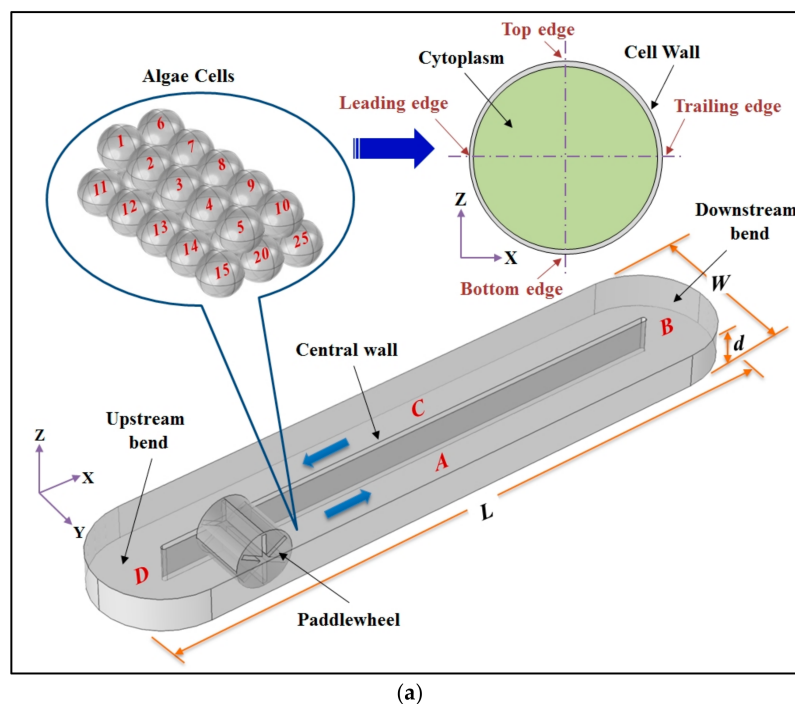
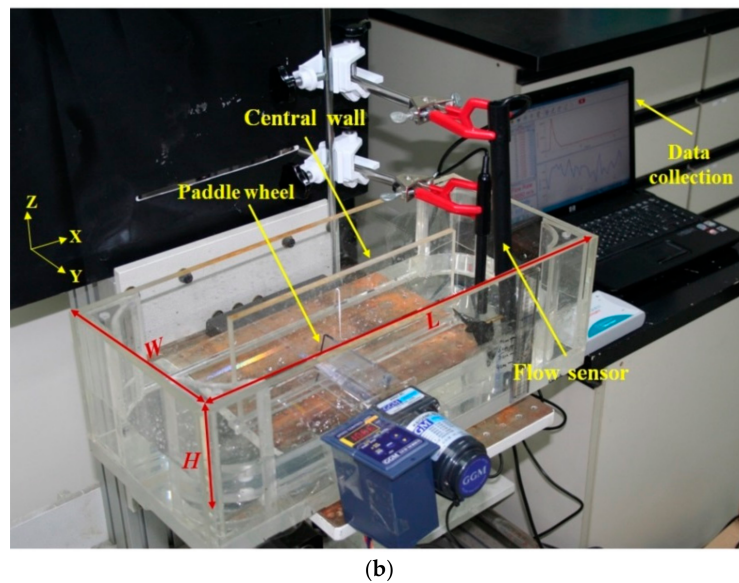


Figure 1. Cont.



**Figure 1.** (a) Computational models of the open raceway pond and microalgal cells used in the simulations and (b) experimental setup with a laboratory-scale raceway pond.

Turbulence magnitude is high near the paddle wheel and low in the downstream bend of a raceway pond [24]. The microalgal cells (*Chlorella*) near the paddle wheel experience larger fluid stress and thus present more cell wall deformation than those in the downstream bend. Therefore, this study thoroughly investigated the effects of turbulence on the cell wall structure by considering four important locations (*A*, *B*, *C*, and *D*) of microalgal cells in the raceway pond (Figure 1a). In real situations, millions of microalgal cells are present in a commercial raceway pond for the mass production of biomass. From the CFD modeling point of view, there is a substantial difference in the dimensions or size of the raceway pond (meters) and the microalgal cells (micrometers) which requires an immense computational meshing and time. Moreover, considering the multiphysics (fluid domain = water flow and cell cytoplasm, solid domain = cell wall) involved in this problem make it more complex. A three-dimensional CFD modeling of fluid–structure interaction (FSI) to investigate the effects of turbulent water flow on millions of the microalgal cells is highly complex and tedious, keeping in view the multidimensional and multiphysics problems. Therefore, a total of 100 spherical microalgal cells (*Chlorella*) were numerically modeled in the raceway pond with distinct cell wall and cytoplasm domains in it. For effective visualization of microalgal cell position and arrangement, only 25 cells are shown in Figure 1a. The diameter of the cytoplasm of *Chlorella* cell is 6.93  $\mu\text{m}$ , and the cell wall thickness is 0.285  $\mu\text{m}$ . This study requires various properties of *Chlorella* cell (cell size, density, viscosity, elastic modulus) to model the effects of water turbulence on the microalgal cell wall. These properties could not be measured because the present study did not cultivate the microalgae (*Chlorella* cells). Therefore, the needed *Chlorella* cell properties were obtained from past experimental studies by Munns et al. [22], Williams and Laurens [31], Wijaya et al. [32], and Jia et al. [33]. The physical, fluid, and structural properties of the spherical microalgal cells (*Chlorella*) are presented in Table 1 [22,31–33]. From a fluid dynamics point of view, four edges (leading, trailing, top, and bottom) of the microalgal cells were defined with respect to flow direction for improved understanding of microalgal cell damage in the raceway pond (Figure 1a). Microalgal cell wall damage was investigated when the microalgal cells reached different locations of the raceway pond (*A*, *B*, *C*, and *D*). The microalgal cells must follow the water flow to effectively interact with nutrients and  $\text{CO}_2$  before reaching the pond's outlet. The Stokes number ( $St$ ) is a widely used non-dimensional number to predict the existence of relative velocity between a fluid and a particle [24,34]. The governing equation of  $St$  can be expressed as follows:

$$St = (\tau_p U_l) / D_h \quad (3)$$

$$\tau_p = (\rho_p d_p^2) / 18\mu_l \quad (4)$$

where  $\tau_p$  is the relaxation time of microalgal cell (s),  $\rho_p$  is the microalgal cell density ( $\text{kg}/\text{m}^3$ ), and  $d_p$  represents the microalgal cell diameter (m). Microalgal cells (*Chlorella*) with the condition ( $St \ll 1$ ) followed the water flow and successfully reached the outlet of the raceway pond [24]. Aspect ratio is a key parameter in open-channel flow systems because it significantly affects the flow characteristics of raceway ponds [35]. Therefore, this study used the non-dimensional aspect ratio ( $AR$ ) to investigate the effects of pond geometry on microalgal cell wall damage in open raceway ponds:

$$AR = \text{Pond width (m)} / \text{Water or pond depth (m)} = W/d \quad (5)$$

This study utilized three different values of  $AR$  (5, 10, and 15) with different water depths and paddle wheel rotational speeds to examine their effects on microalgal cell velocity, wall deformation, and von Misses stress at different positions in the raceway pond.

**Table 1.** Properties of microalgal cells used in the study.

Microalgal Cell	Diameter ( $\mu\text{m}$ )	Thickness ( $\mu\text{m}$ )	Density ( $\text{kg}/\text{m}^3$ )	Viscosity ( $\text{Pa}\cdot\text{s}$ )	Elastic Modulus (MPa)
Cytoplasm	6.93	–	864	0.0052	–
Cell wall	–	0.285	1060	–	8.5

## 2.2. Numerical Modeling

### 2.2.1. Fluid Flow

The study used the ALE method to combine the fluid flow (water and cytoplasm) formulated using an Eulerian description and a spatial frame with solid mechanics (cell wall) formulated using a Lagrangian description and a material (reference) frame. Fluid flow was described by Reynolds-averaged Navier–Stokes (RANS) equations, which provide a solution for the velocity field ( $U_f$ ) of the water and cytoplasm of the microalgal cell. For simplification and reduction of computational time, the intercellular fluid in the microalgal cell was neglected, and the cytoplasm was modeled as a Newtonian viscous fluid [36]. The RANS equations for Newtonian and incompressible fluid flow are as follows:

$$\rho_f \frac{\partial U_f}{\partial t} + \rho_f (U_f \cdot \nabla U_f) + \rho_f (u_f' \otimes \nabla u_f') + (2\rho_f \omega \times U_f) = \nabla \cdot \left[ -p\mathbf{I} + \mu_f (\nabla U_f + (\nabla U_f)^T) \right] - \rho_f (\omega \times (\omega \times r)) + \mathbf{f}_f \quad (6)$$

$$\rho_f (\nabla \cdot U_f) = 0 \quad (7)$$

where  $\rho_f$  is the fluid density ( $\text{kg}/\text{m}^3$ ),  $U_f$  is the time-averaged fluid velocity (m/s),  $\omega$  is the angular velocity of the paddle wheel (rad/s),  $p$  is the fluid pressure (Pa),  $\mathbf{I}$  is the identity matrix,  $u_f'$  is the fluctuating component of velocity (m/s),  $r$  is the position vector,  $\otimes$  is the outer vector product, and  $\mathbf{f}_f$  is the body force on the fluid ( $\text{N}/\text{m}^3$ ). The fluid properties of the cytoplasm used in this study are presented in Table 1 [31].

The  $k$ – $\varepsilon$  turbulence model was used to describe the turbulent flow in the raceway pond. The  $k$ – $\varepsilon$  turbulence model is based on two equations (turbulent kinetic energy ( $k$ ) and dissipation rate of turbulence energy ( $\varepsilon$ )). It is well suited for flows with high Reynolds number due to its stable computations and good convergence rate. The governing equations of turbulent kinetic energy  $k$  and dissipation rate of turbulence energy  $\varepsilon$  for the  $k$ – $\varepsilon$  turbulence model are as follows:

$$\rho_f \frac{\partial k}{\partial t} + \rho_f U_f \cdot \nabla k = \nabla \cdot \left( \left( \mu_f + \frac{\mu_T}{\sigma_k} \right) \nabla k \right) + P_k - \rho_f \varepsilon \quad (8)$$

$$\rho_f \frac{\partial \varepsilon}{\partial t} + \rho_f \mathbf{U}_f \cdot \nabla \varepsilon = \nabla \cdot \left( \left( \mu_f + \frac{\mu_T}{\sigma_\varepsilon} \right) \nabla \varepsilon \right) + C_{\varepsilon 1} \frac{\varepsilon}{k} P_k - C_{\varepsilon 2} \rho_f \frac{\varepsilon^2}{k} \quad (9)$$

$$P_k = \mu_T \left( \nabla \mathbf{U}_f : \left( \nabla \mathbf{U}_f + (\nabla \mathbf{U}_f)^T \right) - \frac{2}{3} (\nabla \cdot \mathbf{U}_f)^2 \right) - \frac{2}{3} \rho_f k \nabla \cdot \mathbf{U}_f \quad (10)$$

where  $\sigma_k$  and  $\sigma_\varepsilon$  are the turbulent Prandtl number for kinetic energy and the dissipation rate, respectively;  $P_k$  is the production term; and  $C_{\varepsilon 1}$  and  $C_{\varepsilon 2}$  are the first and second experimental model constants for the dissipation rate, respectively. The following values to the constants were assigned:  $\sigma_k = 1.0$ ,  $\sigma_\varepsilon = 1.3$ ,  $C_{\varepsilon 1} = 1.44$ ,  $C_{\varepsilon 2} = 1.92$ , and  $C_\mu = 0.09$ . Turbulent or eddy viscosity ( $\mu_T$ ) defined by the  $k$ - $\varepsilon$  turbulence model is as follows:

$$\mu_T = \rho_f C_\mu \frac{k^2}{\varepsilon} \quad (11)$$

where  $\mu_T$  is the turbulent viscosity (Pa-s),  $\varepsilon$  is the turbulent dissipation rate ( $\text{m}^2/\text{s}^3$ ),  $k$  represents the turbulent kinetic energy ( $\text{m}^2/\text{s}^2$ ), and  $C_\mu$  is the model constant. The rotational speed ( $\omega$ ) of the paddle wheel in Equation (6) was modeled using a time-dependent first-order ordinary differential equation as follows:

$$\frac{dN}{dt} = \omega(t) \quad (12)$$

where  $N$  is the number of revolutions per minute (rpm) and  $\omega$  (rad/s) is the angular velocity of the paddle wheel. The paddle wheel rotational speeds were varied from 15 rpm to 30 rpm.

## 2.2.2. Microalgal Cell Wall Structure

A high turbulence magnitude produces large hydrodynamic stresses on microalgal cells, and these stresses damage the cells' mechanical structure (cell wall) [17,37]. Therefore, the cell wall of a spherical microalgal cell (*Chlorella*) was modeled as an elastic structure filled with cytoplasm [33,38]. The governing equation to compute the solid displacement for the microalgal cell wall is as follows:

$$\rho_s \frac{\partial^2 \mathbf{U}_s}{\partial t^2} = \nabla \cdot \boldsymbol{\sigma} + \rho_s \mathbf{f}_s \quad (13)$$

where  $\mathbf{U}_s$  is solid displacement (m),  $\boldsymbol{\sigma}$  is the Cauchy stress tensor in a solid ( $\text{N}/\text{m}^2$ ),  $\rho_s$  is the solid density ( $\text{kg}/\text{m}^3$ ), and  $\mathbf{f}_s$  is the body force components acting on the solid ( $\text{N}/\text{m}^3$ ).  $\boldsymbol{\sigma}$  can be evaluated from the constitutive equation of a Newtonian fluid. Energy is stored in the microalgal cell wall when structural deformation is experienced. This energy is measured in the form of strain energy density function  $W$  as follows:

$$\mathbf{S} = \frac{\partial W}{\partial \boldsymbol{\varepsilon}} \quad (14)$$

where  $\mathbf{S}$  and  $\boldsymbol{\varepsilon}$  are the second Piola–Kirchhoff stress and the Green–Lagrange strain tensor components, respectively. The total force exerted by the fluid on the microalgal cell wall is the negative of the reaction force on the fluid and is represented by the following equation:

$$\mathbf{f}_s = \mathbf{n} \cdot \left\{ -p \mathbf{I} + \left( \mu_f \left( \nabla \mathbf{U}_f + (\nabla \mathbf{U}_f)^T \right) \right) - \frac{2}{3} \mu_f (\nabla \cdot \mathbf{U}_f) \mathbf{I} \right\} \quad (15)$$

where  $\mathbf{U}_f$  is the fluid velocity vector (m/s),  $p$  is the fluid pressure (Pa),  $\mathbf{I}$  is the identity matrix,  $\mathbf{f}_s$  is the body force on the solid ( $\text{N}/\text{m}^3$ ), and  $\mathbf{n}$  is the outward normal to the boundary. RANS equations are solved in the spatial (deformed) frame, whereas structural equations are defined in the material (undeformed) frame. Therefore, transformation of the force is necessary. This transformation is performed by using the following equation:

$$\mathbf{f}_f = \mathbf{f}_s \frac{dv}{dV} \quad (16)$$

where  $f_f$  is the force on the fluid ( $N/m^3$ ),  $f_s$  is the body force acting on the microalgal cell wall ( $N/m^3$ ), and  $dv$  and  $dV$  are the mesh element scale factors for the spatial and material (reference) frames, respectively. The structural properties of the microalgal cell wall used in this study are presented in Table 1 [22,32,33].

### 3. Numerical Simulation and Mesh Generation

The commercial code COMSOL-Multiphysics (V. 5.3) was used to investigate the effects of fluid turbulence on microalgal cell wall damage in the raceway pond. The ALE method was applied to model the effects of water turbulence on the microalgal cell wall structure using the FSI interface of COMSOL. A boundary-connected coupling method was adopted to import the pulsatile flow effects of the 2D paddle wheel into the 3D raceway pond to reduce computation time and memory [24,28–30]. The paddle wheel was modeled with the rotating machinery interface of COMSOL. The computed flow properties of the 2D paddle wheel were provided as inlet flow conditions for the 3D raceway pond. The turbulence flow of the paddle wheel and raceway pond was simulated with the  $k$ - $\epsilon$  turbulence model. A total of 100 spherical microalgal cells were introduced to the raceway pond near the paddle wheel with distinct cell wall and cytoplasm domains. The fluid and structural properties of the microalgal cells were computed when they reached particular locations in the raceway pond ( $A$ ,  $B$ ,  $C$ , and  $D$ ). An implicit transient solver was used to simulate the rotating machinery and FSI interfaces of COMSOL with the  $k$ - $\epsilon$  turbulence model for 200 s at a time step of 0.001 s. The 2D paddle wheel was discretized with a free triangular mesh, whereas the 3D raceway pond and microalgal cells were discretized with a free tetrahedral mesh. Moreover, a boundary layer mesh with dense element distribution was used along the FSI boundaries of microalgal cells to compute the flow fields in these regions accurately. A grid independency test was performed to determine the accuracy of the present ALE methodology. Water velocity was measured in the middle ( $Y$ -axis) of the downstream bend of the raceway pond (Figure 2a). The wall deformation of the microalgal cell (cell 3) was estimated in location  $A$  in the raceway pond and is shown in Figure 2b. The results were computed in a raceway pond with  $AR = 10$ , water depth = 0.2 m, and paddle wheel rotational speed = 20 rpm. Three different mesh sizes, namely, fine, extra-fine, and extremely-fine, were adopted in this study and varied with a factor of five. Detailed information on the mesh elements used in this study is provided in Table 2. A minimal difference was observed between the results of water velocity magnitude and cell wall deformation (Figure 2). Therefore, all simulations in this study were performed using the extra-fine mesh element size.

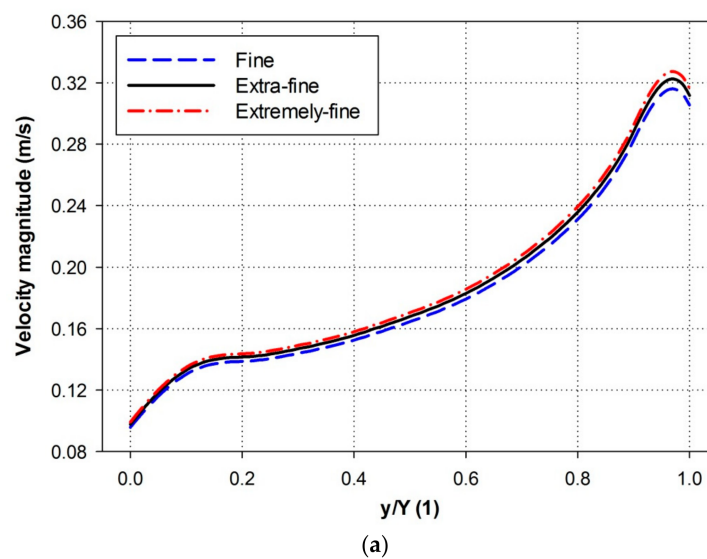


Figure 2. Cont.

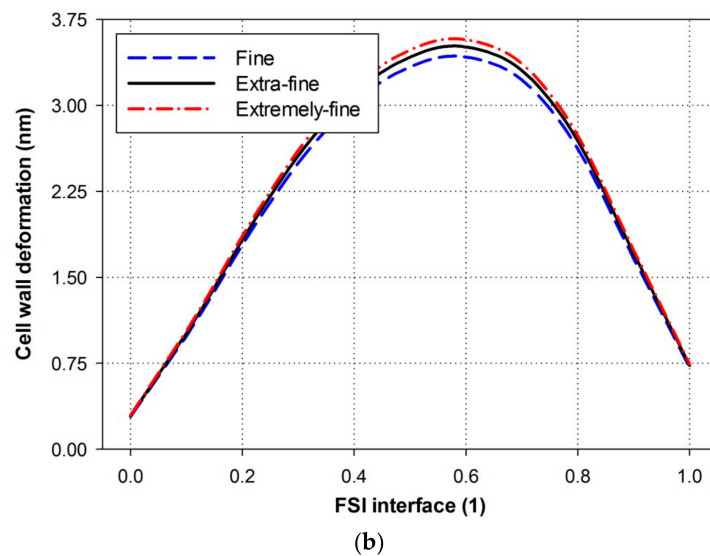


Figure 2. Grid independency test using (a) water velocity (m/s) and (b) cell wall deformation (nm).

Table 2. Mesh elements of the paddle wheel, raceway pond, and microalgal cells.

Geometries	Elements	Fine	Extra-Fine	Extremely-Fine
Paddle wheel	Domain	4334	21,670	108,350
	Boundary	561	2805	14,025
Raceway pond and microalgal cells	Domain	111,429	557,145	2,785,725
	Boundary	33,360	166,800	834,000
	Edge	6480	32,400	162,000

## 4. Results and Discussion

### 4.1. Experimental Comparison

An experiment was also conducted in another laboratory-scale raceway pond to compare and validate the proposed numerical ALE methodology based on water velocity (Figure 3). *Chlorella* was not cultivated in the experimental raceway pond since it was beyond the scope of the present study. The experiment was performed in a laboratory-scale raceway pond with a length ( $L$ ) of 0.5 m, width ( $W$ ) of 0.2 m, and height ( $H$ ) of 0.15 m (Figure 1b). Water depth ( $d$ ) was maintained at 0.05 m during the experiment. A paddle wheel (diameter = 0.1 m) with six blades (0.1 m  $\times$  0.025 m) was used to generate pulsatile flow in the raceway pond. An AC induction motor (60 Hz) with a maximum rotational speed of 240 and a gear ratio of 7.5:1 was used to rotate the paddle wheel. Water velocity (m/s) was measured with a flow rate sensor (FLO-BTA, Vernier, Beaverton, OR, USA). The flow rate sensor was connected to a computer using the LabQuest stream (Vernier) interface, and time-dependent flow velocity was recorded.

Water velocity (m/s) was estimated experimentally and numerically in the middle ( $Y$ -axis) of the downstream bend of raceway pond at a paddle wheel rotational speed of 35 rpm (Figure 3a). The velocity near the central wall was significantly lower than that at the side wall of the raceway pond. This phenomenon implied the formation of a dead zone that decreased microalgal production because of the accumulation of microalgal cells in these regions [21]. The numerical results matched the experimentally calculated water velocity, thereby verifying the proposed ALE methodology. Water velocity (m/s) was also computed under various time intervals in the middle ( $Y$ -axis) of the downstream bend to further compare the results of the present numerical methodology with the experimental results (Figure 3b). A sudden increase in water velocity was observed at the start of the experiment because of the flow instability caused by the paddle wheel movement. However, the water flow in the pond

became stable with the passage of time and resulted in a uniform water velocity. A reasonable agreement was observed between the experimental and numerical results, thereby confirming that the proposed numerical ALE methodology can be adopted to simulate turbulence effects on microalgal cell wall damage in raceway ponds.

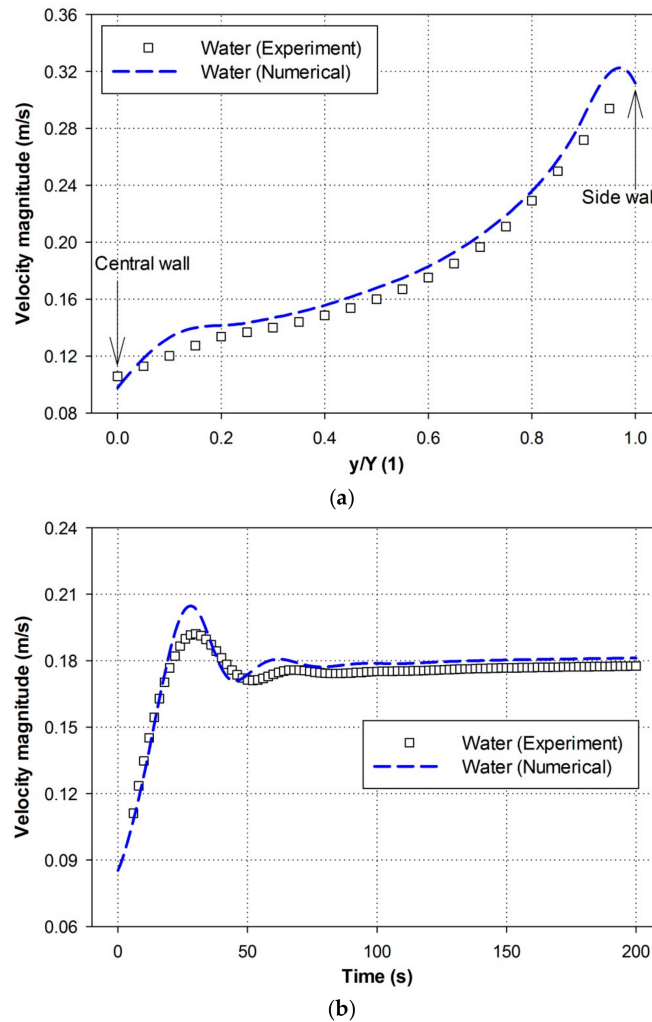
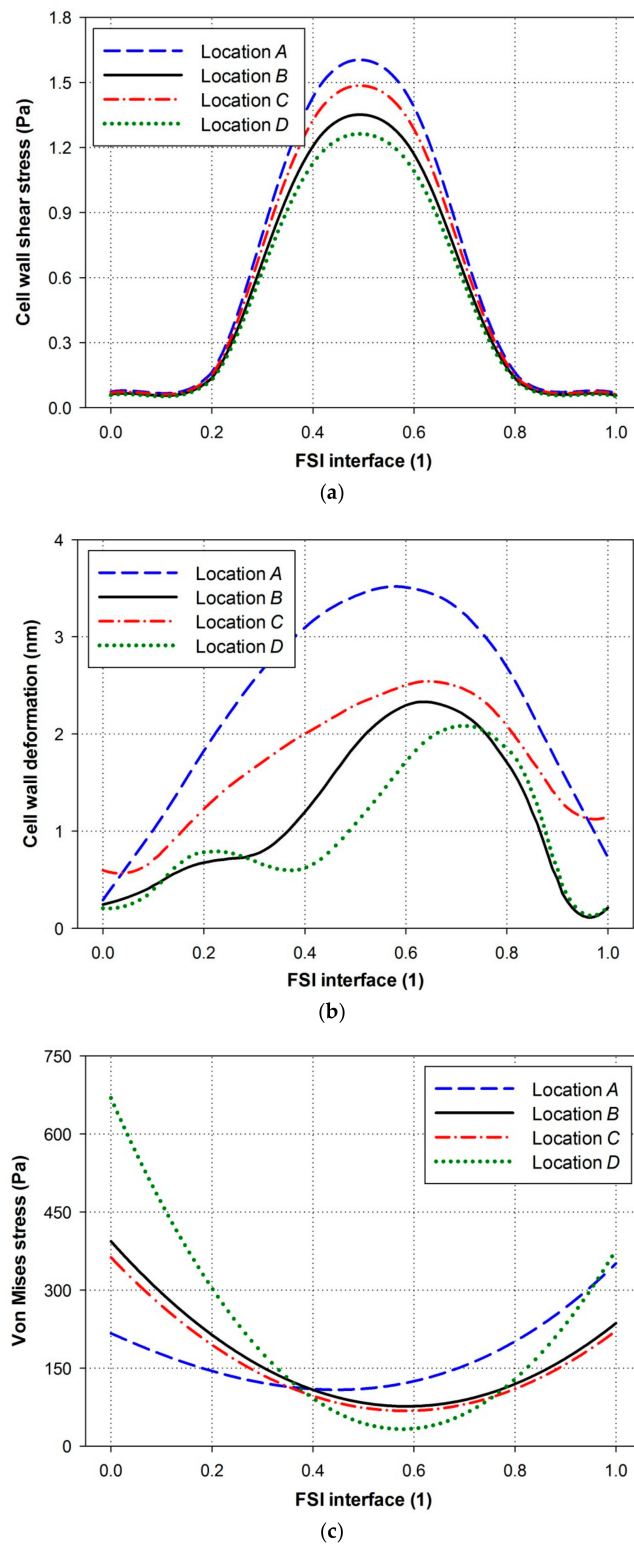


Figure 3. Comparison of experimental and CFD results on velocity magnitude (m/s).

#### 4.2. Effects of Microalgal Cell Locations

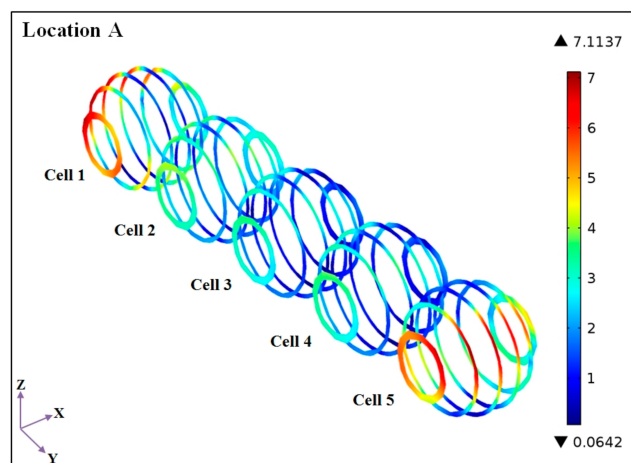
Turbulent flow mixing was high near the paddle wheel and significantly decreased as the water flowed from the upstream to the downstream bend of the raceway pond. Therefore, the mechanical properties of the cell wall were estimated at different locations (*A*, *B*, *C*, and *D*) in the raceway pond to investigate turbulence effects on microalgal cell wall damage. The effect of different locations of microalgal cells on cell wall shear stress (Pa), cell wall deformation (nm), and von Mises stress (Pa) is presented in Figure 4. The results were computed in a raceway pond with  $AR = 10$ , water depth = 0.2 m, and paddle wheel rotational speed = 20 rpm. The properties were computed on the FSI interface (bottom, leading, and top edges) of microalgal cell 3. The wall shear stress on the surface of the microalgal cell was computed to investigate nutrient diffusivity. Cell wall shear stress was high at the leading edge and low at the remaining edges of the microalgal cell (Figure 4a). Wall shear stress increased significantly at locations *A* and *C* because of highly turbulent mixing. This finding implies that nutrient diffusivity increases at locations *A* and *C* because of the reduced boundary layers around the cell surface caused by high shear stress.



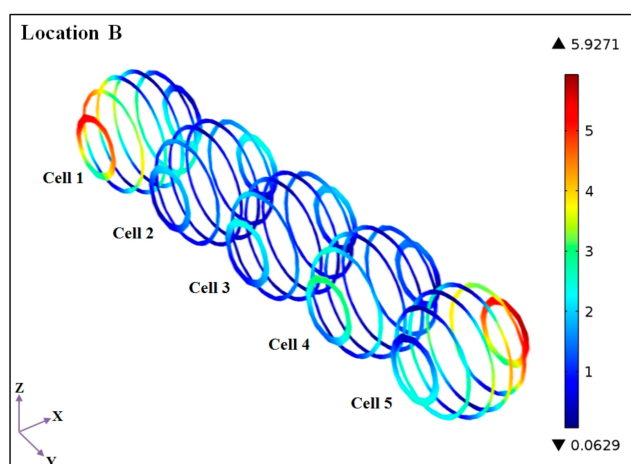
**Figure 4.** Effect of different locations of microalgal cells in the raceway pond on (a) cell wall shear stress (Pa); (b) wall deformation (nm); and (c) von Mises stress (Pa).

The microalgal cell wall showed more deformation in the leading edge region than in the regions of the bottom and top edges (Figure 4b). The interaction of microalgal cells with one another helped reduce the effect of flow stresses on the cell walls, as evidenced by the low deformation at the top and

bottom edges. The maximum deformation in cell wall was recorded at location *A* because of the highly turbulent flow in this pond region. Cell wall deformation was low when the microalgal cells were in the downstream and upstream bends (locations *B* and *D*). Von Mises stress showed an inverse relationship with cell wall deformation (Figure 4c). The minimum von Mises stress was observed at the leading edge of the microalgal cells, and the maximum was observed at the top and bottom edges because large fluid forces induce high stresses on the cell wall. The maximum von Mises stress at location *A* showed that the microalgal cell exhibited high resistance to cell wall deformation, whereas the minimum von Mises stress at the remaining locations (*B*, *C*, and *D*) indicated low resistance to wall deformation. These results suggest that the leading edge of microalgal cells is considerably fragile, especially when the microalgal cells are near the paddle wheel (location *A*), which may affect algal productivity [17,37]. Contour plots of the cell wall deformation (nm) of five microalgal cells were created at various locations in the raceway pond to visualize microalgal cells damage effectively (Figure 5). The wall deformation of microalgal cells present in the middle (i.e., 2, 3, and 4) was low because of sufficient interaction with adjacent microalgal cells (i.e., 1 and 5). However, the microalgal cells at the corners (i.e., 1 and 5) experienced large wall deformation because of minimal contact with the adjacent cells. Turbulent mixing was increased in the return channel (location *C*) of the raceway pond due to the large secondary flows in the downstream bend [24]. Therefore, cell wall deformation was at the maximum when the microalgal cell moved in location *C* of the raceway pond (Figure 5c). The deformation of the microalgal cell walls was at the minimum in the upstream bend (location *D*) because of the reduced turbulent mixing (Figure 5d).

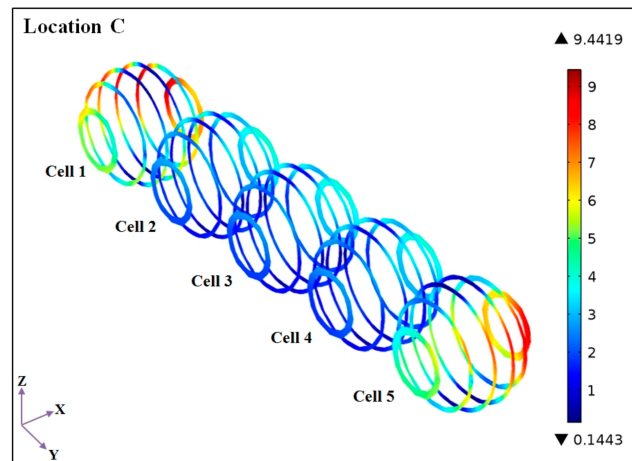


(a)

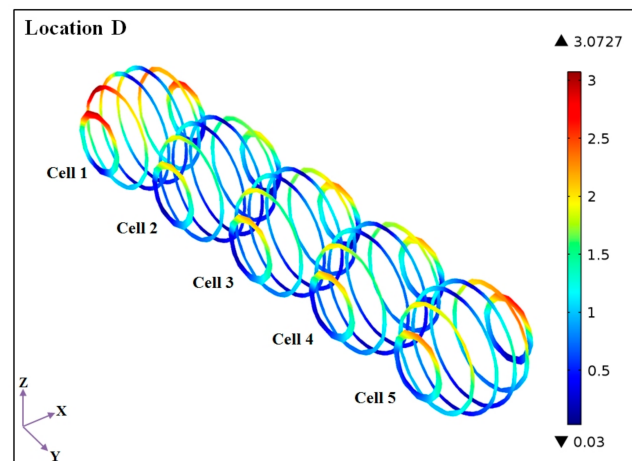


(b)

Figure 5. Cont.



(c)



(d)

**Figure 5.** Contour plots of microalgal cell wall deformation (nm) for a raceway pond with  $AR = 10$  at a water depth of 0.2 m and rotational speed of 20 (rpm). (a) location A; (b) location B; (c) location C and (d) location D.

Contour plots ( $YZ$  plane) of the cell wall deformation (nm) of microalgal cell 3 were also created at various locations in the raceway pond (Figure 6). The shape of the microalgal cell wall was significantly deformed from its original position at location A because of the increased turbulent mixing (Figure 6a). This deformation in the structural shape of the cell wall can destroy the microalgal cell by damaging its inner structure (nucleus, chloroplast, etc.). Similarly, the microalgal cell at location C experienced this deformation in its wall structure shape (Figure 6b). These findings imply that locations A and C are critical to microalgal productivity because microalgal cell damage is likely to occur in these pond areas [16,18]. Therefore, this study used microalgal cell 3 at location C to further examine (following sections) the effects of the pond's geometrical and hydrodynamic properties on the microalgal cell damage. All the results in the following sections were plotted on the  $XZ$  plane.

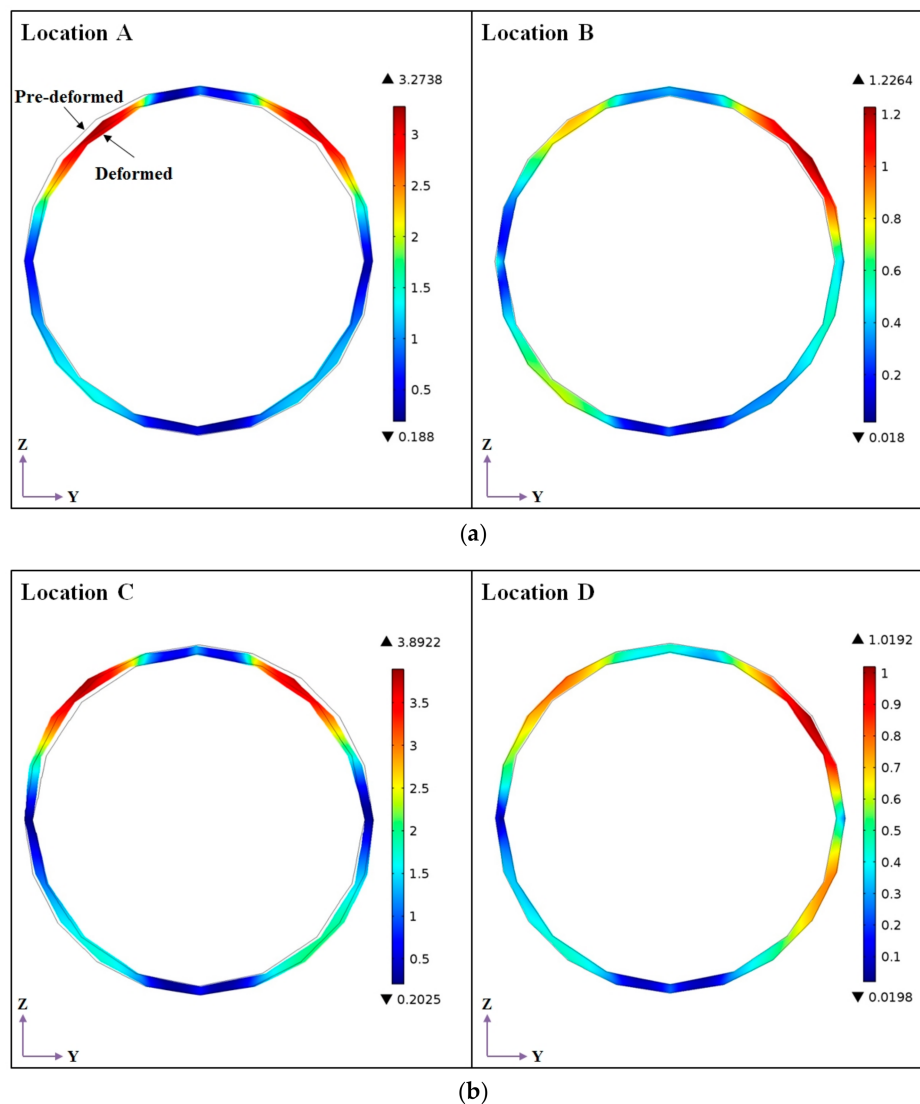


**Figure 6.** Contour plots (YZ plane) of wall deformation (nm) of microalgal cells in a raceway pond with  $AR = 10$  at a water depth of 0.2 m and rotational speed of 20 (rpm). (a) locations A and B; (b) locations C and D.

#### 4.3. Effects of Aspect Ratio

The effect of different  $AR$ s on the radial wall deformation (nm) and von Mises stress (Pa) of the microalgal cell in a raceway pond with a water depth of 0.2 m and paddle wheel rotational speed of 20 is shown in Figure 7. The cell wall deformation (nm) of the microalgal cell decreased with the increase in  $AR$  because of the reduction in turbulent mixing (Figure 7a). The paddle wheel rotational speed was kept constant, which increased  $AR$ , reduced the water velocity in the raceway pond, and consequently decreased the turbulent mixing. Therefore, raceway ponds with high  $AR$  experience small secondary flows, which decrease the cell wall deformation due to the small applied fluid stresses [24,39]. A maximum decrease of about 8.5% in cell wall deformation was recorded with the increase in  $AR$  from 5 to 10, whereas a 10% decrease in cell wall deformation was found when  $AR$  was increased from 10 to 15. The effect of different  $AR$ s on the radial von Mises stress (Pa) of the microalgal cells in the raceway pond is shown in Figure 7b. This study used the radial von Mises stress to determine whether the cell wall of the microalgal cells will sustain the applied turbulence flow forces. The von Mises stress was significantly reduced with the increase in the  $AR$  of the raceway

pond. An increase in  $AR$  from 5 to 10 resulted in a maximum decrease of about 11% in von Mises stress, whereas an 9% decrease was found with the increase in  $AR$  from 10 to 15. These results suggest that turbulent mixing is effective in raceway ponds with small  $AR$ s; it increases sunlight distribution and nutrient diffusion to the microalgal cell surface. However, narrow raceway ponds (small  $AR$ s) result in large cell wall deformations, which indicate the possibility of substantial damage on microalgal cells, and thus reduce cell productivity [15,17,19,20].

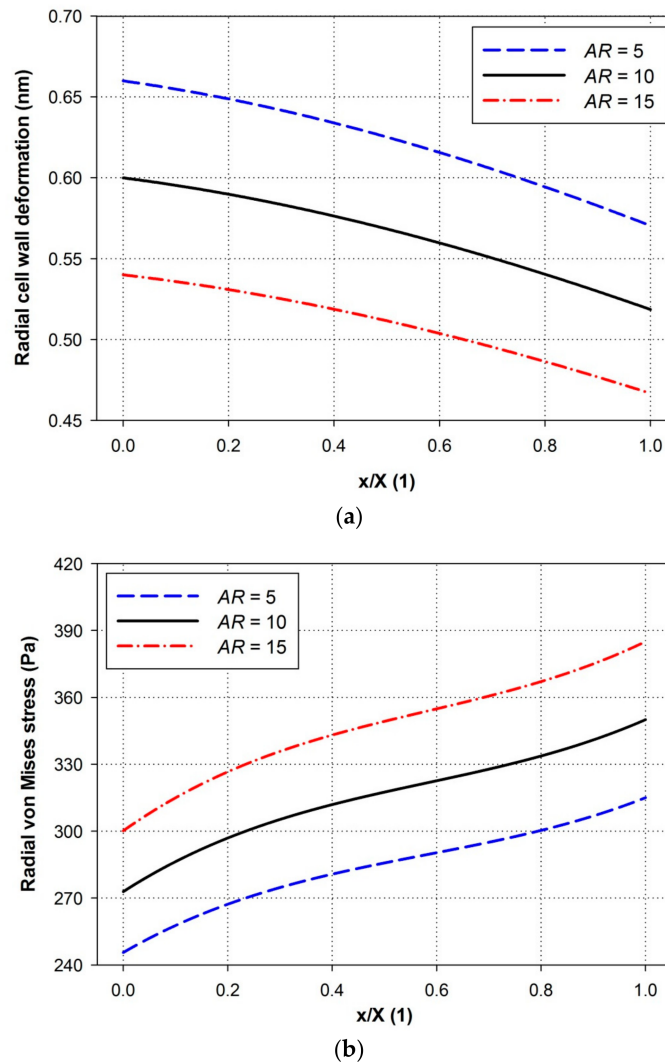


**Figure 7.** Effect of  $AR$ s on radial (a) cell wall deformation (nm) and (b) von Mises stress (Pa).

#### 4.4. Effects of Water Depths

Microalgal cell wall damage is affected significantly by water depth because of its direct influence on turbulent mixing in a raceway pond. Therefore, the effects of water depth on the wall deformation (nm) and von Mises stress (Pa) of the microalgal cell in a raceway pond with a  $AR = 10$  and paddle wheel rotational speed = 20 (rpm) were estimated and are presented in Figure 8. Water depth showed an inverse relationship with cell wall deformation of the microalgal cell (Figure 8a). A decrease in water depth resulted in a significant increase in cell wall deformation because of the increase in the turbulent mixing in the raceway pond. Cell wall deformation decreased by about 16% with the increase in water depth from 0.1 m to 0.2 m. The pond depth of 0.3 m recorded a decrease of 29% in the cell wall deformation of the microalgal cell. Raceway ponds with small water depths allow sunlight to penetrate to the pond's bottom and facilitate uniform mixing of microalgal cells for effective light utilization [2–4].

The effect of water depth on the von Mises stress (Pa) of the microalgal cells is shown in Figure 8b. Water depth exerted a significant effect on the magnitudes of the von Mises stress. Increasing the water depth also resulted in a decrease in von Mises stress because of small hydrodynamic fluid forces. Von Mises stress showed a maximum decrease of about 31% when the water depth was increased from 0.1 m to 0.2 m. However, a decrease of 39% in von Mises stress was recorded for the 0.3 m water depth. These findings imply that microalgal cells present in shallow raceway ponds are prone to damage because of large cell wall deformations, which destroy the microalgal culture and consequently reduce biomass productivity [16–18].

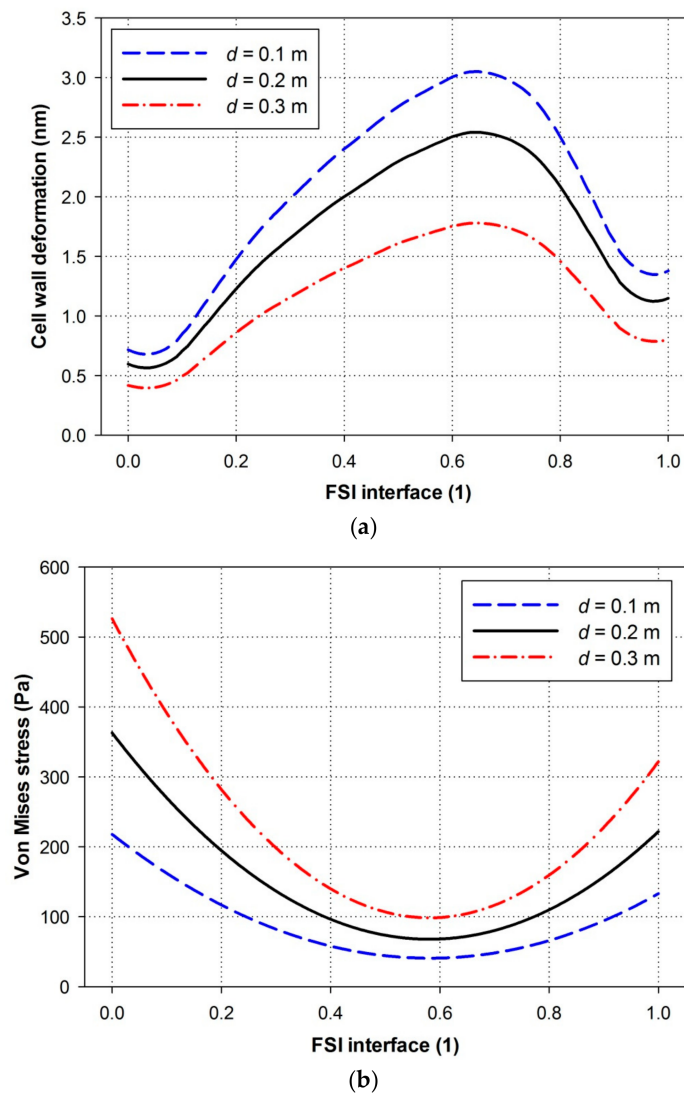


**Figure 8.** Effect of water depths on (a) cell wall deformation (nm) and (b) von Mises stress (Pa).

#### 4.5. Effects of Paddle Wheel Rotational Speeds

Turbulent mixing directly depends on paddle wheel rotational speeds, and turbulence mixing can be increased by increasing the speeds of the paddle wheel. The effects of paddle wheel rotational speeds on the radial wall deformation (nm) and von Mises stress (Pa) of the microalgal cells in a raceway pond with a  $AR = 10$  and water depth = 0.2 m were measured (Figure 9). Cell wall deformation was directly related to paddle wheel rotational speed. An increase in paddle wheel rotational speed increased the turbulent mixing, which consequently increased cell wall deformation by applying increased hydrodynamic stresses (Figure 9a). A maximum increase of approximately

15% in wall deformation was recorded when the paddle wheel rotational speed was increased from 15 rpm to 20 rpm. Meanwhile, increasing the paddle wheel speed from 25 rpm to 30 rpm resulted in a maximum increase in cell deformation by about 13%. High paddle wheel rotational speeds may reduce the boundary layer around the microalgal cells to improve nutrient diffusivity. However, the microalgal cell wall was largely deformed because of the large fluid forces produced at high paddle wheel rotational speeds (Figure 9a). The effect of paddle wheel rotational speeds on the radial von Mises stress (Pa) of the microalgal cells was also evaluated and is presented in Figure 9b. The von Mises stress increased significantly with an increase in the paddle wheel speeds because of the large hydrodynamic stresses on the microalgal cells. An increase of approximately 12% in von Mises stress was recorded with each increase in the paddle wheel rotational speed (i.e., 15 rpm to 20 rpm and 25 rpm to 30 rpm). These results suggest that high paddle wheel rotational speeds certainly damage the mechanical structure of microalgal cells. Therefore, high paddle wheel rotational speeds are unsuitable for microalgal cultivation in raceway ponds because of the large deformation of the microalgal cell wall and high power requirement [16,17].

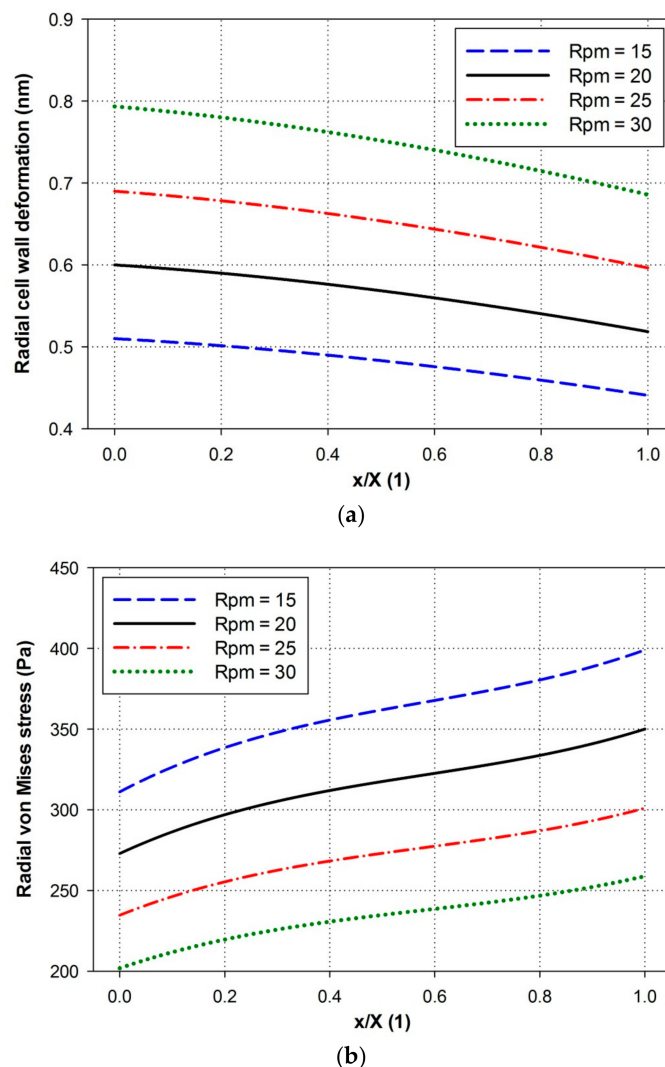


**Figure 9.** Effect of paddle wheel rotational speeds (rpm) on radial (a) microalgal cell deformation (nm) and (b) von Mises stress (Pa).

## 5. Conclusions

This study developed a FSI-based numerical model to investigate the effects of water turbulence on microalgal cell wall damage in open raceway ponds. The ALE numerical methodology was adopted to model the effects of water turbulence on the microalgal cell wall. Microalgal cell wall damage was investigated at four different locations in the raceway pond in consideration of the effects of pond's hydrodynamic and geometric properties. The numerical results were compared and validated using the experimental time-dependent water velocity. Various aspect ratios, water depths, and paddle wheel rotational speeds were considered to examine their effects on microalgal cell wall shear stress, cell wall deformation, and von Mises stress at different locations in the raceway pond.

The nutrient diffusivity rate to microalgal cells increased at locations A and C because of high cell wall shear stresses, which consequently reduced the boundary layer around the cell surface. The portion of microalgal cells having first contact with the water flow deformed more compared with the others. The particle–particle interaction of microalgal cells helped reduce the effect of flow stresses on their cell wall structure. Cell wall shear stress showed a direct relationship with cell wall deformation, whereas von Mises stress is inversely related to cell wall deformation. Locations A and C are critical in terms of microalgal cell wall damage, which suggests that algal productivity may be significantly affected in these pond regions. An increasing AR decreased the microalgal cell wall deformation and the von Mises stresses. Wide raceway pond channels are thus suitable for algal cultivation because of reduced cell wall damage. The cell wall deformation and von Mises stresses also decreased with an increase in water depth. Microalgal cell wall damage was high in the raceway ponds with small water depths. Increasing the paddle wheel speeds also significantly increased the cell wall deformation and von Mises stresses. High paddle wheel rotational speeds reduced algal productivity because of an increase in microalgal cell wall damage. Therefore, appropriate selection of hydrodynamic and geometric properties must be made to achieve effective turbulent mixing with reduced microalgal cell wall damage for optimizing algal productivity.

**Acknowledgments:** This study was supported by a National Research Foundation of Korea (NRF) grant funded by the Korea government (MSIP) (No. 2017R1A2B2005515), and a grant from the Priority Research Centers Program through the NRF, as funded by the MEST (No. 2010-0020089).

**Author Contributions:** H.A. conceived and designed the simulations and experiments; H.A. performed the simulations and experiments; T.A.C. designed the paper structure and analyzed the results; C.W.P. gave suggestions and made corrections in the paper; H.A. wrote the paper.

**Conflicts of Interest:** The authors declare no conflict of interest.

## References

1. Borowitzka, M.A. Commercial production of microalgae: Ponds, tanks, tubes and fermenters. *J. Biotechnol.* **1999**, *70*, 313–321. [[CrossRef](#)]
2. Grobbelaar, J.U.; Kroon, B.M.A.; Burger-Wiersma, T.; Mur, L.R. Influence of medium frequency light/dark cycles of equal duration on the photosynthesis and respiration of *Chlorella pyrenoidosa*. *Hydrobiologia* **1992**, *238*, 53–62. [[CrossRef](#)]
3. Marshall, J.S.; Huang, Y. Simulation of light-limited algae growth in homogeneous turbulence. *Chem. Eng. Sci.* **2010**, *65*, 3865–3875. [[CrossRef](#)]
4. Schapira, M.; Seuront, L.; Gentilhomme, V. Effects of small-scale turbulence on *Phaeocystis globosa* (Prymnesiophyceae) growth and life cycle. *J. Exp. Mar. Biol. Ecol.* **2006**, *335*, 27–38. [[CrossRef](#)]
5. Silva, H.J.; Cortifas, T.; Ertola, R.J. Effect of hydrodynamic stress on *dunaliella* growth. *J. Chem. Technol. Biotechnol.* **2007**, *40*, 41–49. [[CrossRef](#)]
6. Blersch, D.M.; Kangas, P.C.; Mulbry, W.W. Turbulence and nutrient interactions that control benthic algal production in an engineered cultivation raceway. *Algal Res.* **2013**, *2*, 107–112. [[CrossRef](#)]
7. Barbosa, M.J.; Albrecht, M.; Wijffels, R.H. Hydrodynamic stress and lethal events in sparged microalgae cultures. *Biotechnol. Bioeng.* **2003**, *83*, 112–120. [[CrossRef](#)] [[PubMed](#)]

8. Baldyga, J.; Pohorecki, R. Influence of turbulent mechanical stresses on microorganisms. *Appl. Mech. Rev.* **1998**, *51*, 121–140. [[CrossRef](#)]
9. Ogbonna, J.C.; Yada, H.; Tanaka, H. Effect of cell movement by random mixing between the surface and bottom of photobioreactors on algal productivity. *J. Ferment. Bioeng.* **1995**, *79*, 152–157. [[CrossRef](#)]
10. Weissman, J.C.; Goebel, R.P.; Benemann, J.R. Photobioreactor design: Mixing, carbon utilization, and oxygen accumulation. *Biotechnol. Bioeng.* **1988**, *31*, 336–344. [[CrossRef](#)] [[PubMed](#)]
11. Bosca, C.; Dauta, A.; Marvalin, O. Intensive outdoor algal cultures: How mixing enhances the photosynthetic production rate. *Bioresour. Technol.* **1991**, *38*, 185–188. [[CrossRef](#)]
12. Chisti, Y. Biodiesel from microalgae. *Biotechnol. Adv.* **2007**, *25*, 294–306. [[CrossRef](#)] [[PubMed](#)]
13. Mendoza, J.L.; Granados, M.R.; de Godos, I.; Ación, F.G.; Molina, E.; Heaven, S.; Banks, C.J. Oxygen transfer and evolution in microalgal culture in open raceways. *Bioresour. Technol.* **2013**, *137*, 188–195. [[CrossRef](#)] [[PubMed](#)]
14. Drapcho, C. The partitioned aquaculture system: Impact of design and environmental parameters on algal productivity and photosynthetic oxygen production. *Aquac. Eng.* **2000**, *21*, 151–168. [[CrossRef](#)]
15. Grobbelaar, J.U. The influence of light/dark cycles in mixed algal cultures on their productivity. *Bioresour. Technol.* **1991**, *38*, 189–194. [[CrossRef](#)]
16. Thomas, W.H.; Gibson, C.H. Effects of small-scale turbulence on microalgae. *J. Appl. Phycol.* **1990**, *2*, 71–77. [[CrossRef](#)]
17. Camacho, F.G.; Gómez, A.C.; Sobczuk, T.M.; Grima, E.M. Effects of mechanical and hydrodynamic stress in agitated, sparged cultures of *Porphyridium cruentum*. *Process Biochem.* **2000**, *35*, 1045–1050. [[CrossRef](#)]
18. Berdalet, E.; Peters, F.; Koumandou, V.L.; Roldan, C.; Guadayol, O.; Estrada, M. Species-specific physiological response of dinoflagellates to quantified small-scale turbulence. *J. Phycol.* **2007**, *43*, 965–977. [[CrossRef](#)]
19. Hondzo, M.; Lyn, D. Quantified small-scale turbulence inhibits the growth of a green alga. *Freshw. Biol.* **1999**, *41*, 51–61. [[CrossRef](#)]
20. Al-Homoud, A.; Hondzo, M. Energy dissipation estimates in oscillating grid setup: LDV and PIV measurements. *Environ. Fluid Mech.* **2007**, *7*, 143–158. [[CrossRef](#)]
21. Hadiyanto, H.; Elmore, S.; Van Gerven, T.; Stankiewicz, A. Hydrodynamic evaluations in high rate algae pond (HRAP) design. *Chem. Eng. J.* **2013**, *217*, 231–239. [[CrossRef](#)]
22. Munns, R.; Greenway, H.; Setter, T.L.; Kuo, J. Turgor pressure, volumetric elastic modulus, osmotic volume and ultrastructure of *Chlorella emersonii* grown at high and low external NaCl. *J. Exp. Bot.* **1983**, *34*, 144–155. [[CrossRef](#)]
23. Secomb, T.W.; Hsu, R.; Pries, A.R. Blood Flow and Red Blood Cell Deformation in Nonuniform Capillaries: Effects of the Endothelial Surface Layer. *Microcirculation* **2002**, *9*, 189–196. [[CrossRef](#)] [[PubMed](#)]
24. Ali, H.; Cheema, T.A.; Yoon, H.-S.; Do, Y.; Park, C.W. Numerical prediction of algae cell mixing feature in raceway ponds using particle tracing methods. *Biotechnol. Bioeng.* **2015**, *112*, 297–307. [[CrossRef](#)] [[PubMed](#)]
25. Mendoza, J.L.; Granados, M.R.; de Godos, I.; Ación, F.G.; Molina, E.; Banks, C.; Heaven, S. Fluid-dynamic characterization of real-scale raceway reactors for microalgae production. *Biomass Bioenergy* **2013**, *54*, 267–275. [[CrossRef](#)]
26. Duarte, F.; Gormaz, R.; Natesan, S. Arbitrary Lagrangian-Eulerian method for Navier-Stokes equations with moving boundaries. *Comput. Methods Appl. Mech. Eng.* **2004**, *193*, 4819–4836. [[CrossRef](#)]
27. Clair, G.; Ghidaglia, J.-M.; Perlat, J.-P. A multi-dimensional finite volume cell-centered direct ALE solver for hydrodynamics. *J. Comput. Phys.* **2016**, *326*, 312–333. [[CrossRef](#)]
28. Ali, H.; Cheema, T.A.; Park, C.W. Effect of Paddle-Wheel Pulsating Velocity on the Hydrodynamic Performance of High-Rate Algal Ponds. *J. Energy Eng.* **2015**, *141*, 4014039. [[CrossRef](#)]
29. Ali, H.; Cheema, T.A.; Park, C.W. Numerical prediction of heat transfer characteristics based on monthly temperature gradient in algal open raceway ponds. *Int. J. Heat Mass Transf.* **2017**, *106*, 7–17. [[CrossRef](#)]
30. Ali, H.; Park, C.W. Numerical multiphase modeling of CO<sub>2</sub> absorption and desorption in microalgal raceway ponds to improve their carbonation efficiency. *Energy* **2017**, *127*, 358–371. [[CrossRef](#)]
31. Williams, P.J.L.B.; Laurens, L.M.L. Microalgae as biodiesel & biomass feedstocks: Review & analysis of the biochemistry, energetics & economics. *Energy Environ. Sci.* **2010**, *3*, 554. [[CrossRef](#)]
32. Wijaya, F.B.; Mohapatra, A.R.; Sepehrirahnama, S.; Lim, K.M. Coupled acoustic-shell model for experimental study of cell stiffness under acoustophoresis. *Microfluid. Nanofluid.* **2016**, *20*, 69. [[CrossRef](#)]

33. Jia, F.; Ben Amar, M.; Billoud, B.; Charrier, B. Morphoelasticity in the development of brown alga *Ectocarpus siliculosus*: From cell rounding to branching. *J. R. Soc. Interface* **2017**, *14*. [[CrossRef](#)] [[PubMed](#)]
34. Lucci, F.; Ferrante, A.; Elghobashi, S. Is Stokes number an appropriate indicator for turbulence modulation by particles of Taylor-length-scale size? *Phys. Fluids* **2011**, *23*, 25101. [[CrossRef](#)]
35. Auel, C.; Albayrak, I.; Boes, R.M. Turbulence Characteristics in Supercritical Open Channel Flows: Effects of Froude Number and Aspect Ratio. *J. Hydraul. Eng.* **2014**, *140*, 4014004. [[CrossRef](#)]
36. Wolff, K.; Marenduzzo, D.; Cates, M.E. Cytoplasmic streaming in plant cells: The role of wall slip. *J. R. Soc. Interface* **2012**, *9*, 1398–1408. [[CrossRef](#)] [[PubMed](#)]
37. Papoutsakis, E.T. Fluid-mechanical damage of animal cells in bioreactors. *Trends Biotechnol.* **1991**, *9*, 427–437. [[CrossRef](#)]
38. Stenson, J.D.; Thomas, C.R.; Hartley, P. Modelling the mechanical properties of yeast cells. *Chem. Eng. Sci.* **2009**, *64*, 1892–1903. [[CrossRef](#)]
39. Simionato, D.; Basso, S.; Giacometti, G.M.; Morosinotto, T. Optimization of light use efficiency for biofuel production in algae. *Biophys. Chem.* **2013**, *182*, 71–78. [[CrossRef](#)] [[PubMed](#)]



© 2018 by the authors. Licensee MDPI, Basel, Switzerland. This article is an open access article distributed under the terms and conditions of the Creative Commons Attribution (CC BY) license (<http://creativecommons.org/licenses/by/4.0/>).